Core ideas:

- Finite probe effects of HP sensors with dissimilar probe properties are quantified.
- The finite probe effects on HP signals are most significant in dry soils.
- Errors resulting from finite probe properties can be eliminated by using the CPC theory.
- Finite probe size and properties should be considered in HP sensor design.

Application of infinite line source and cylindrical-perfect-conductor theories to heat pulse measurements with large sensors

Wei Peng [a], Yili Lu [a, *], Tusheng Ren [a], Robert Horton [b]

a College of Land Science and Technology, China Agricultural University, Beijing, China 100193

b Department of Agronomy, Iowa State University, Ames, IA 50011

* Corresponding author: luyili@cau.edu.cn

ABSTRACT

The infinite line source (ILS) theory for soil thermal property determination with heat pulse (HP) sensors is simple and widely-used, but ignores the finite probe radius (*r*) and heat capacity (C_p). The cylindrical-perfect-conductors (CPC) theory, which accounts for *r* and C_p by using the identical-cylindrical-perfect-conductors (ICPC) or the dissimilar-cylindrical-perfect-conductors (DCPC) approaches, can be applied to estimate soil thermal property values with improved accuracy. In this study, the ILS and CPC theories were evaluated, and the finite *r* and C_p effects were quantified using numerical simulations and laboratory measurements with a large HP sensor of dissimilar probes. The errors due to finite probe properties were saturation dependent: Dry soils had a 14% reduction in the maximum temperature rise of the HP signal, while only slight temperature differences occurred in wet sandy soils. The finite probe effects were minor on ICPC- and DCPC-thermal property values with relative errors generally less than 5%, but the absolute values of relative errors for dry soils were greater than 6%. Errors caused by ignoring the finite probe effects changed linearly with the ratio of soil *C* versus *C* of the heating and sensing probes. The dissimilar probe *r* had negligible effect on HP signals and thermal property estimates with the specific sensor used in this study. The effects of finite probe size and properties should be considered in HP sensor design. The CPC theory is recommended for estimating soil thermal properties with large HP sensors.

Abbreviations: HP, Heat pulse; ILS, Infinite line source; CPC, Cylindrical-perfect-conductors; ICPC, Identical-cylindrical-perfect-conductors; DCPC, Dissimilar-cylindrical-perfect-conductors.

INTRODUCTION

The heat pulse (HP) technique has been widely used to measure soil thermal properties and other soil physical properties under laboratory and field conditions (He, Dyck, Horton, Ren, Bristow, Lv, & Si, 2018; Peng, Lu, Xie, Ren, & Horton, 2019; Tian, Ren, Horton, & Heitman, 2020). A HP sensor consists of heating and sensing probes that are aligned in parallel. The sensing probe measures soil temperature response-with-time data (HP signals) aft er release of a short-duration heat-pulse from the heating probe. Soil thermal properties are derived from the HP measurements.

A common approach for soil thermal property estimation is the infinite line source (ILS) theory that assumes sensor probes to have infinite length and zero diameter (Campbell, Calissendorff, & Williams, 1991; Bristow, Kluitenberg, & Horton, 1994; Knight & Kluitenberg, 2015; Liu, Lu, Wen, Ren, & Horton, 2020). The ILS theory, however, is subject to errors because it ignores the finite probe properties, such as the thermal properties and cylindrical geometry (Kluitenberg, Ham, & Bristow, 1993; Kluitenberg, Bristow, & Das, 1995; Liu, Li, Ren, & Horton, 2007). Knight, Kluitenberg, Kamai, & Hopmans (2012) presented a cylindrical-perfect-conductors (CPC) theory with a semi-analytical solution that accounted for the finite probe radius (r) and finite probe heat capacity (C_p). They provided an example analysis where the heating and sensing probes had identical r and C_p (hereafter identical-cylindrical-perfect-conductors, ICPC), and showed that r and C_p could cause significant changes in the timing and magnitude of HP signals, especially in dry soils. Lu, Wang, & Ren (2013) found that compared to the ILS theory, the ICPC theory could effectively reduce the overestimation errors in HP-measured specific heat capacity of soil solids. For field applications, large-size HP sensors (e.g., with probe length of 45~70 mm, and diameter of 2~2.38 mm) have been designed to improve the probe rigidity. These large HP sensors, in combination with the ICPC theory, provided more accurate soil heat capacity (C) and water content (θ) estimates than those from small-size probes with the ILS theory, by reducing errors from probe deflection and finite probe properties (Kamai, Kluitenberg, & Hopmans, 2015).

Peng et al. (2019) introduced a HP sensor design (hereafter Peng-type sensor) that had dissimilar diameters for the heating and sensing probes. Compared to other HP sensors, the Peng-type sensor had the advantages of improved probe rigidity, sharpened probe tips and thinner sensing probes to minimize soil disturbance during insertion, thus reduced the changes of probe spacing during sensor deployment under field conditions. With its robust and long needles, the

Peng-type sensor could also be used to measure soil water content with the technique of time domain reflectometry. However, Peng et al. (2019) ignored the presence of dissimilar probes in estimating soil thermal properties following the ICPC theory. A general CPC theory is required to quantify the errors resulting from dissimilar probe properties. Furthermore, the Knight et al. (2012) CPC theory assumed that the sensing probe did not interfere with the radial symmetry of temperature distribution around the heating probe. Theoretical analysis has shown that for dual-probe HP sensors with considerations of finite r and C_p, there exist interactions between the heating and sensing probes, i.e., the temperature field around the heating probe may be altered by the sensing probe, depending on the probe size (Knight, Kluitenberg, & Kamai, 2016). Thus, there is a need to further examine the accuracy of soil thermal property values obtained with large-size HP sensors with dissimilar probes.

The objectives of this study are to evaluate the ILS and CPC theories for sensors with dissimilar heating and sensing probes by using numerical simulations and laboratory experiments, and to quantify the effects of finite probe properties on HP signals and soil thermal property estimates by using the Peng-type sensor as an example. Potential implications of the results on HP sensor design are also discussed.

THEORY

The solution for radial conduction of a short-duration heat pulse away from an ILS (Kluitenberg et al., 1993; Bristow et al., 1994) is,

$$T(R,t)=\begin{cases}\dfrac{-q'}{4\pi C\alpha}\mathrm{Ei}\left(\dfrac{-R^2}{4\alpha t}\right);0<t\le t_0\\ \dfrac{q'}{4\pi C\alpha}\left\{\mathrm{Ei}\left[\dfrac{-R^2}{4\alpha\left(t-t_0\right)}\right]-\mathrm{Ei}\left(\dfrac{-R^2}{4\alpha t}\right)\right\};t>t_0\end{cases} \quad [1]$$

where -Ei(-x) is the exponential integral, q' is the rate per unit length at which heat is released from the heating probe, C is soil heat capacity, α is soil thermal diffusivity, t_0 is the duration of the heat pulse, t is the measurement time, R is the spacing between the heating and sensing probes, and T (R, t) is the temperature at the sensing probe.

Knight et al. (2012) derived a semi-analytical solution that considered the finite r and C_p values of the HP probes. A special case of the CPC solution, with identical heating and sensing probes, is the ICPC solution. For the case of continuous heating, a Laplace transform expression of the sensing probe temperature at a known distance from the centerline of the infinite cylindrical heat source is,

$$\hat{V}(p) = \hat{v}_f^2(p, r_0, \beta_0)\frac{q'K_0(\mu R)}{2\pi\lambda p} \quad [2]$$

where λ is soil thermal conductivity; r_0 is the radius of heating and sensing probes, and β_0 = C_{p0}/C, where C_{p0} is the heat capacity of the heating and sensing probes in ICPC solution; $K_u(z)$ denotes the modified Bessel function of the second kind of order u and argument z; $\mu = \sqrt{p/\alpha}$, where p is the Laplace transform parameter; $\hat{V}(p)$ is the Laplace transform of $V(t)$, which is the temperature of the sensing probe, and $\hat{v}_f(p, r_0, \beta_0)$ is the corresponding transfer function.

For a HP sensor with heating and sensing probes having different r and C_p values, the CPC solution is defined as dissimilar-cylindrical-perfect-conductors (DCPC). For the case of continuous heating, the general solution in the Laplace transform domain for the temperature of the sensing probe is formulated as,

$$\hat{V}(p) = \hat{v}_f(p, r_1, \beta_1)\hat{v}_f(p, r_2, \beta_2)\frac{q'K_0(\mu R)}{2\pi\lambda p} \quad [3]$$

where r_1 and r_2 are the radii of the heating and sensing probes, respectively; β_1 = C_{p1}/C and β_2 =

C_{p2}/C, where C_{p1} is volumetric heat capacity of the heating probe, and C_{p2} is the heat capacity of the sensing probe. The transfer function for the heating probe is,

$$\hat{v}_f(p, r_1, \beta_1) = \frac{1}{\mu r_1[K_1(\mu r_1) + (\mu r_1 \beta_1 / 2) K_0(\mu r_1)]} \quad [4]$$

and the transfer function for the sensing probe is,

$$\hat{v}_f(p, r_2, \beta_2) = \frac{1}{\mu r_2[K_1(\mu r_2) + (\mu r_2 \beta_2 / 2) K_0(\mu r_2)]} \quad [5]$$

According to Knight et al. (2012), Eq. [3] can be numerically inverted using the algorithm of Stehfest (1970a, b) to solve for the sensing probe temperature values of $V(t)$ and $V(t\text{-}t_0)$ for the case of a pulsed heating scheme. Then, the temperature of the sensing probe is obtained by using the principle of superposition in time and substituting $V(t)$ and $V(t\text{-}t_0)$ into the following expression (Knight et al., 2012),

$$V^p(t) = \begin{cases} V(t); 0 < t \le t_0 \\ V(t) - V(t - t_0); t > t_0 \end{cases} \quad [6]$$

Eqs. [2] and [6] formulate the semi-analytical ICPC solution for temperature changes at the sensing probe, while Eqs. [3] and [6] formulate the semi-analytical DCPC solution for temperature changes at the sensing probe.

The above solution can be used to estimate soil thermal properties by fitting Eq. [6] in the form of the Stehfest inversion ($t > t_0$) to the measured temperature-by-time data, with specific probe configurations and properties as inputs. The algorithm used to evaluate the DCPC solution is nearly identical to that used for the ICPC solution, except the term $\hat{v}_f^2(p, r_0, \beta_0)$ in Eq. [2] is replaced with $\hat{v}_f(p, r_1, \beta_1)$ and $\hat{v}_f(p, r_2, \beta_2)$.

For a HP sensor with dissimilar probes, the probe heat capacities C_{p1} and C_{p2} can be estimated with the following equations,

$$C_{p1} = C_E \frac{a_{eh}^2}{r_1^2} + C_{SS}(1 - \frac{a_{eh}^2}{r_1^2}) \qquad [7]$$

$$C_{p2} = C_E \frac{a_{es}^2}{r_2^2} + C_{SS}(1 - \frac{a_{es}^2}{r_2^2}) \qquad [8]$$

where C_E is the volumetric heat capacity of the thermally conductive epoxy that is filled into the probes, C_{SS} is the volumetric heat capacity of stainless steel, a_{eh} and a_{es} are the radius values of the epoxy-filled region of the heating probe and sensing probe, respectively. The physical characteristics and properties of the probe materials for the Peng-type sensor are listed in Tables 1 and 2. The estimated C_{p0} value used in the ICPC solution is 3.42 MJ m^{-3} K^{-1}, and the estimated C_{p1} and C_{p2} values are 3.42 and 2.57 MJ m^{-3} K^{-1} used in DCPC solution, respectively, according to Eqs. [7]-[8].

MATERIALS AND METHODS

To clarify the effects of finite probe properties on HP signals, numerical experiments were performed to obtain the simulated temperature change-by-time curves, and laboratory measurements were conducted on soil samples to acquire real HP signals. Soil thermal properties were estimated by fitting the ILS and CPC solutions to the HP data, and then comparisons of ILS- and CPC-soil thermal property values were performed to quantify the errors due to finite probe properties. The factors β_0 and β_2 were used to characterize the finite and dissimilar probe effects on soil thermal property estimations, respectively.

Numerical simulations with COMSOL Multiphysics

For the numerical simulation scheme, the problem domain was a cylindrical region with a radius of 35 mm and a length of 80 mm with zero initial temperature distribution and an adiabatic boundary condition. We adopted the Peng-type sensor configuration and assumed that there was no thermal contact resistance at the probe-soil interface. We considered that the HP sensor had only one heater probe and one sensing probe, and a thermocouple (located at the mid-length position) was used to sense temperature.

Three simulation scenarios, i.e., NP, IP, and DP, were designed to represent the ILS, ICPC and DCPC theories, respectively. The NP scenario considered an infinite line as a heat source, with the simulated temperature values at an R distance from the line source without considering probe r and C_p (Fig. 1a). For the IP scenario, identical r and C_p values of the heating and sensing probes were considered (Fig. 1b). For the DP scenario, the r and C_p values of the heating and sensing probes were dissimilar (Fig. 1c). The heating and sensing probes were treated as composite solids that consisted of stainless-steel tubing filled with thermally conductive epoxy with known C and λ values (Table 2). We used the 3D transient heat conduction module of COMSOL Multiphysics finite-element software (Version 5.4a, COMSOL) to simulate the temperature change-by-time data for the NP, IP and DP scenarios.

To quantify the effects of probe r and C_p on HP signals, a hypothetical, homogeneous, isotropic sandy soil (94% sand, 1% silt, 5% clay) was used in the simulation. The hypothetical soil solids had a specific heat capacity of 0.742 kJ kg^{-1} K^{-1}. The soil bulk density (ρ_b) was set at 1.60 Mg m^{-3}, and four θ values (0.00, 0.10, 0.20, and 0.30 m^3 m^{-3}) were used, with a corresponding C range of 1.19-2.44 MJ m^{-3} K^{-1} and a λ range of 0.34-1.87 W m^{-1} K^{-1}, which were estimated by using the de Vries (1963) C model and the Lu, Lu, Horton, & Ren (2014) λ model, respectively. The parameters for the heating scheme (duration and intensity) were kept constant for all the scenarios (Table 1).

Laboratory HP measurements

Laboratory experiments were performed to obtain HP signals (the temperature change-by-time data) on repacked soil cores using the Peng-type sensor, from which soil *C*, α, and λ were estimated by fitting the ILS (Eq. [1]), ICPC (Eqs. [2] and [6]), and DCPC (Eqs. [3] and [6]) solutions to the measured HP data. First, the HP signals were determined in agar-immobilized water (5 g L^{-1}) at 20°C to calibrate *R* (Zhang, Lu, Ren, & Horton, 2020). Then *R* values were estimated by fitting the ILS, ICPC and DCPC solutions to the above HP signals with the MATLAB software (The Math Works, Inc., Natick, MA), assuming a heat capacity of 4.18 MJ m^{-3} K^{-1} for the agar-immobilized water (Campbell et al., 1991). Soils with sand (94% sand, 1% silt, 5% clay) and loam (48% sand, 38% silt, 14% clay) textures were used in the measurements. The soil samples were air-dried, passed through a 2-mm sieve, and packed into cylinders (35×80 mm) at approximate θ values of 0.00, 0.05, 0.10, 0.15, 0.20, 0.25, and 0.30 m^3 m^{-3} at a room temperature of 20±1°C. The ρ_b values ranged from 1.50 to 1.68 Mg m^{-3} for the sand soil, and from 1.19 to 1.35 Mg m^{-3} for the loam soil. Please refer to Peng et al. (2019) for details of soil thermal property measurements with the HP method. Following the HP measurements, the soil cores were oven dried at 105°C to obtain the actual θ and ρ_b values.

Error analysis

Soil thermal property values obtained from the ILS and ICPC solutions were compared to values estimated from the DCPC solution. The relative error (*RE*) and root mean square error (*RMSE*) were calculated,

$$RE = \frac{x_i - x_d}{x_d} \times 100\% \qquad [9]$$

$$RMSE = \sqrt{\frac{\sum (x_i - x_d)^2}{n}} \qquad [10]$$

where x_i represents the soil thermal property values derived from the ILS or ICPC solution, x_d represents values estimated by the DCPC solution. For *RE* calculations, the specific x_i and x_d term are listed in Figs. 4 and 5. *n* is the number of data points.

RESULTS AND DISCUSSION

Effects of probe *r* and C_p on simulated temperature with time curves

Figure 2 shows the COMSOL simulated temperature-by-time curves from the Peng-type sensor on the hypothetical sandy soil under the NP, IP and DP scenarios. The effects of finite probe properties on the temperature curve varied considerably with θ, as manifested in the maximum temperature change (ΔT_{max}). For the dry soil (θ = 0 m^3 m^{-3}), ΔT_{max} values under the three scenarios were in the order of NP (~1.14°C), DP (~1.03°C), and IP (~1°C) (Fig. 2a). Under moist conditions (θ from 0.10 to 0.30 m^3 m^{-3}), two distinct features were observed in the maximum temperature differences (Figs. 2b, 2c, and 2d). First, ΔT_{max} values of the DP and IP scenarios generally agreed well with each other; secondly, the NP scenario had slightly larger ΔT_{max} values than those of the DP and IP scenarios, and the differences were reduced at wetter conditions (e.g., ΔT_{max} differences between NP and DP were 0.06°C at θ of 0.10 m^3 m^{-3} and 0.02°C at θ of 0.30 m^3 m^{-3}). Additionally, the HP signals of the NP scenario had earlier arrival times than those of the DP and IP scenarios. Thus, it could be concluded that (1) In dry soils, the dissimilar probe effects (i.e., differences between DP and IP scenarios) on ΔT_{max} were minor compared with the finite probe effects (i.e., differences among NP and DP or IP scenarios); (2) the finite probe effects on ΔT_{max} faded as θ increased; and (3) the dissimilar probe effects on ΔT_{max} were negligible in wet soils with $\theta \geq$ 0.1 m^3 m^{-3}. Also, with the DP scenario (r_2 = 2 mm), it was observed that the presence of a sensing probe did not significantly alter the simulated temperature of the heating probe (data not shown). When r_2 was increased to 2.38 mm (IP scenario), a change in the temperature distribution around the heating probe started to manifest, but it still had a negligible effect on the temperature field. This implied that the probe sizes (i.e., r values) of both the heating and sensing probes should be considered in HP sensor design and construction.

These saturation-dependent finite probe effects were in line with the reports of Knight et al. (2012) and Lu et al. (2013). Under dry conditions, when soil C and C_p had the maximum difference, heat absorption by the heating probes accounted for a significant portion of the HP signals, which caused a delayed arrival time and a lower $\Delta T_{\max}$ at the sensing probe. Thus, ignoring the finite probe r resulted in an earlier arrival time and larger HP signals. For the Peng-type sensor, the effects of dissimilar probe C_p values were observable in dry soils only. To obtain the same temperature rise, more energy was needed for the IP sensing probe than for the DP sensing probe, because of the larger C_{p2} in the IP scenario. As a result, the $\Delta T_{\max}$ arrived later, and its magnitude was decreased (Fig. 2a). The differences between IP- and DP-HP signals were induced by the finite probe properties of the sensing probes.

Soil thermal property estimates with the ILS, ICPC and DCPC approaches

Figure 3 shows the comparisons of C, α and λ estimates with the DCPC approach versus those from the ILS and ICPC approaches. For both sand and loam soils, the ILS theory yielded relatively large C values (with an average *RMSE* of 0.056 MJ m^{-3} K^{-1}, Fig. 3a) and lower α values (with an average *RMSE* of 0.378×10^{-7} m^{2} s^{-1}, Fig. 3b), but relatively accurate λ values (Fig. 3c). In contrast, the C, α and λ values derived with the ICPC approach agreed well with those from the DCPC approach, as indicated by the relatively low *RMSE*s and evenly scattered data points near the 1:1 line (Figs. 3d, 3e, and 3f). The errors in ILS estimated C and α values were caused by ignoring the finite r and C_p of the probes and thus a significant increment of $\Delta T_{\max}$ at the sensing probe. It was apparent that the finite probe effects had less influence on λ than on C and α estimates.

To further quantify the effects of finite probe r and C_p on ILS, ICPC and DCPC estimated soil thermal properties, we compared the *RE*s of ILS- and ICPC-C, α and λ values against the DCPC derived values (Fig. 4). Compared to the DCPC approach, the *RE*s of ILS-estimated C, α and λ values were 4%, -6% and -3%, which indicated an overestimation of C and underestimation of α and λ values on both soils across all θ values (Figs. 4a, 4b, and 4c). The corresponding *RE*s of ICPC-estimated C, α and λ values were -2%, 4% and 2% for C, α and λ values (Figs. 4d, 4e, and 4f), respectively, about 30% to 50% lower than those of the ILS approach. In addition, the absolute *RE* values showed decreasing trends with increasing θ, especially for the results from the ILS approach. For example, the largest errors were observed for θ values less than 0.10 m^3 m^{-3}, where the *RE*s were as high as 7%, -12%, and -6% for ILS-estimated C, α and λ values, respectively (Figs. 4a, 4b, and 4c). At θ > 0.10 m^3 m^{-3}, the overall *RE*s of the ILS-estimated C were less than 3%, and the ILS-estimated α and λ had absolute *RE*s less than 6%. The *RE*s of the ICPC-estimated soil thermal properties were generally within ±5% for the entire water range.

The finite probe effects on soil thermal property estimates with the HP sensors were further evaluated by using parameter β, the ratio between soil heat capacity C and probe heat capacity C_p. For ICPC theory, β_0 was defined to represent the effects of finite probe properties, which was the major difference between ILS and ICPC. In DCPC theory, β_1 and β_2 were designated to represent the effects of the heating and sensing probes, respectively, in which β_1 was equal to β_0. When calculating β, soil C values were estimated from θ and ρ_b values of the soil cores by using the de Vries (1963) model, and C_p was calculated with Eqs. [7] and [8] by considering r and C values of all probe materials. The results showed that with increasing β_0, the *RE*s of ILS-estimated thermal property values increased either positively (C) or negatively (α and λ) (Fig. 5a). For example, when β_0 changed from 2 to 3, or the heating probe C_p was about 2 to 3 times that of soil C, the corresponding *RE*s changed from 5% to 9% for C, -8% to -16% for α, and -4% to -8% for λ. Regression analysis indicated strong linear relationships between β_0 and *RE* values, with coefficients of determination (R^2) greater than 0.96. The same trend could be found for the ICPC-thermal properties. As overall ICPC-*RE*s were reducing to ~5%, linear relationships between *RE* and β_2 were observed with R^2 over 0.95 (Fig. 5b). This means that the change in β_2 (finite property of sensing probes) introduced no more than ±5% in thermal property estimates. Overall, it implies that β_0 and β_2 values can be used as indictors for finite probe effect characterization for HP sensor designs, and ignoring properties of heating probes induces errors in soil thermal property estimates.

In this study, our analysis on the effects of dissimilar probe properties is performed based on the Peng-type sensor. The methodology can also be applied to other sensor configurations. A thicker heating probe (e.g., r_1 = 2.38~4 mm and r_2 = 2 mm) will produce a greater r_1/r_2 ratio, leading to a larger C_{p1} = 3.42~3.65 MJ m^{-3} K^{-1} and C_{p2} = 2.57 MJ m^{-3} K^{-1} (Eqs. [7] and [8]), and thus a greater reduction in $\Delta T_{\max}$ and a further arrival time delay in the HP signals. For the sand soil, when the r_1/r_2 is increased to 2, the $\Delta T_{\max}$ is 0.07°C in a dry sample, but reduces to 0.01°C in wet samples. Thus, the effects of dissimilar probe properties are significant for dry soils, and it is important to consider both the finite probe size and properties for future HP sensor designs.

CONCLUSIONS

In this study, numerical simulations and laboratory measurements were used to quantify the effects of finite probe properties on HP signals, and to evaluate the performance of the ILS and CPC solutions applied to a large HP sensor with dissimilar probes. The simulation results demonstrated that the finite probe effects on temperature rise with time curves were significant in dry soils, and were weak in wet soils. While thermal property estimates with the ILS theory had absolute values of *RE*s greater than 6%, the ICPC approach had *RE*s generally less than 5%. The factors of β_0 and β_2 were useful for characterizing the finite probe errors on soil thermal property estimates. For large

HP sensors, the CPC solution gave accurate soil thermal property estimations. For sensors having dissimilar probes, the DCPC theory was a viable option to derive accurate *C*, α, and λ values from the HP temperature-by-time data. Although the dissimilar probe *r* had negligible effects on HP signals and thermal property estimates for the specific sensor used in this study, the effects of finite probe size and property should be considered in future HP sensor designs.

ACKNOWLEDGEMENTS

This research was funded by the National Natural Science Foundation of China (41977011 and 41671223), the U.S. National Science Foundation (1623806) and USDA-NIFA Multi-State Project 4188. The authors gratefully acknowledge the help of Dr. Gerard Kluitenberg (Kansas State University) for the helpful comments on implementing the CPC theory and the MATLAB scripts. The MATLAB code for the CPC solution is available upon request from the corresponding author (luyili@cau.edu.cn).

REFERENCES

Bristow, K.L., Kluitenberg, G.J., & Horton, R. (1994). Measurement of soil thermal properties with a dual-probe heat-pulse technique. Soil Science Society of America Journal, 58, 1288-1294.

Campbell, G.S., Calissendorff, K., & Williams, J.H. (1991). Probe for measuring soil specific heat using a heat-pulse method. *Soil Science Society of America Journal*, 55, 291-293.

de Vries, D.A. (1963). Thermal properties of soils. In: W. R. Van Wijk, editor, *Physics of plant environment*. North-Holland Publ. Co., Amsterdam.

He, H.L., Dyck, M.F., Horton, R., Ren, T.S., Bristow, K.L., Lv, J.L., & Si, B.C. (2018). Development and application of the heat pulse method for soil physical measurements. *Reviews of Geophysics*, 56, 567-620.

Knight, J.H., Kluitenberg, G.J., & Kamai, T. (2016). The dual probe heat pulse method: interaction between probes of finite radius and finite heat capacity. *Journal of Engineering Mathematics*, 99(1):79-102.

Knight, J.H., & Kluitenberg, G.J. (2015). A simple rational approximation for heat capacity determination with the dual-probe heat-pulse method. *Soil Science Society of America Journal*, 79, 495-498.

Kamai, T., Kluitenberg, G.J., & Hopmans, J.W. (2015). A dual-probe heat-pulse sensor with rigid probes for improved soil water content measurement. *Soil Science Society of America Journal*, 79:1059-1072.

Knight, J.H., Kluitenberg, G.J., Kamai, T., & Hopmans, J.W. (2012). Semianalytical solution for dual-probe heat-pulse applications that accounts for probe radius and heat capacity. *Vadose Zone Journal*, 11(2).

Kluitenberg, G.J., Bristow, K.L., & Das, B.S. (1995). Error analysis of heat pulse method for measuring soil heat capacity, diffusivity, and conductivity. *Soil Science Society of America Journal*, 59, 719-726.

Kluitenberg, G.J., Ham, J.M., & Bristow, K.L. (1993). Error analysis of the heat pulse method for measuring soil volumetric heat capacity. *Soil Science Society of America Journal*, 57, 1444-1451.

Liu, G., Lu, Y.L., Wen, M.M., Ren, T.S., & Horton, R. (2020). Advancing in the heat-pulse technique: Improvements in measuring soil thermal properties. *Soil Science Society of America Journal*, 84, 1361-1370.

Lu, Y.L., Lu, S., Horton, R., & Ren, T.S. (2014). An empirical model for estimating soil thermal conductivity from texture, water content, and bulk density. *Soil Science Society of America Journal*, 78, 1859-1868.

Lu, Y.L., Wang, Y.J., & Ren, T.S. (2013). Using late time data improves the heat-pulse method for estimating soil thermal properties with the pulsed infinite line source theory. *Vadose Zone Journal*, 12(4).

Liu, G., Li, B.G., Ren, T.S. & Horton, R. (2007). Analytical solution of heat pulse method in a parallelepiped sample space. *Soil Science Society of America Journal*, 71,1607-1619.

Peng, W., Lu, Y.L., Xie, X.T., Ren, T.S., & Horton, R. (2019). An improved thermo-TDR technique for monitoring soil thermal properties, water content, bulk density, and porosity. *Vadose Zone Journal*, 18, 190026.

Stehfest, H. (1970a). Algorithm 368: Numerical inversion of Laplace transforms. *Communications of ACM*, 13, 47-49.

Stehfest H. (1970b). Remark on Algorithm 368: Numerical inversion of Laplace transforms. *Communications of ACM*, 13, 624.

Tian, Z.C., Ren, T.S., Horton, R., & Heitman, J.L. (2020). Estimating soil bulk density with combined commercial soil water content and thermal property sensors. *Soil & Tillage Research*, 196, 104445.

Zhang, M, Lu, Y.L., Ren, T.S., & Horton, R. (2020). In-situ probe spacing calibration improves the heat pulse method for measuring soil heat capacity and water content. *Soil Science Society of America Journal*, 84, 1620-1629.

Figure Captions List

Figure 1. Schematic diagrams of the COMSOL simulations: (a) the scenario with finite probe radius (r) and heat capacity (C_p) ignored (NP); (b) the scenario with identical r and C_p values of heating and sensing probes (IP); (c) the scenario with dissimilar r and C_p values for heating and sensing probes (DP). Parameter R is the distance between the centers of heating and sensing probes, r_0 is the IP probe radius, r_1 and r_2 are the radii of the DP heater and sensing probes, respectively, and a_{eh} and a_{es} are the radii of the epoxy filled regions in the heating and sensing probes, respectively. All of the parameter values are listed in Table 1.

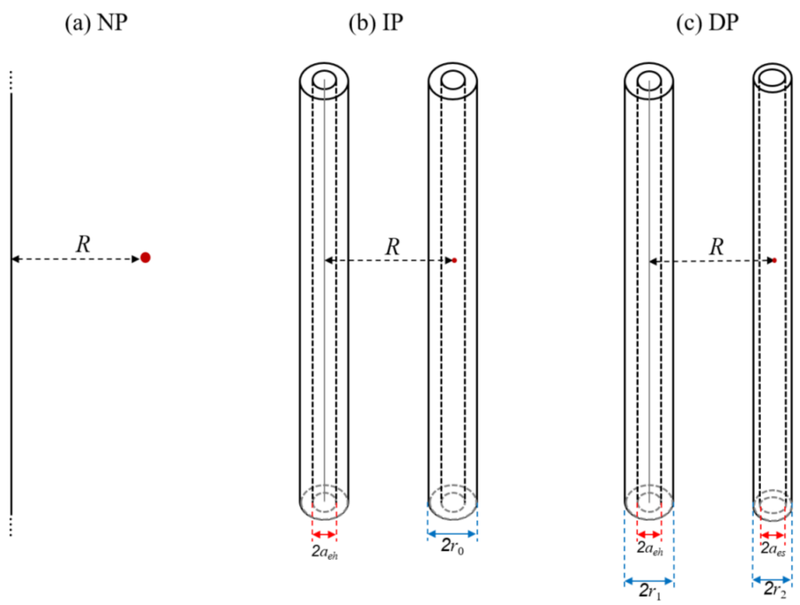

Figure 2. Simulated temperature change-by-time curves of a hypothetical sandy soil at four water contents (θ) under the scenario with finite probe radius (*r*) and heat capacity (C_p) ignored (NP); the scenario with identical *r* and C_p values of heating and sensing probes (IP); and the scenario with dissimilar *r* and C_p values for heating and sensing probes (DP).

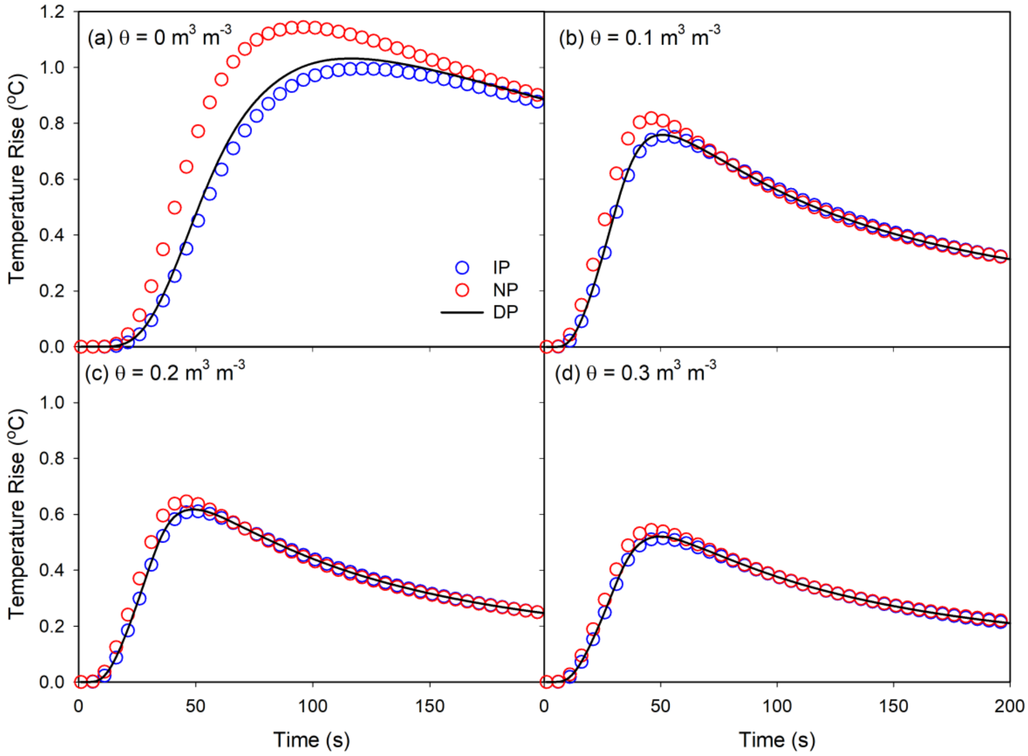

Figure 3. Comparison of soil heat capacity (*C*), thermal diffusivity (α) and thermal conductivity (λ) estimated with the infinite line source (ILS) and the identical-cylindrical-perfect-conductors (ICPC) approaches vs. those with the dissimilar-cylindrical-perfect-conductors (DCPC) approach for a sand soil and a loam soil.

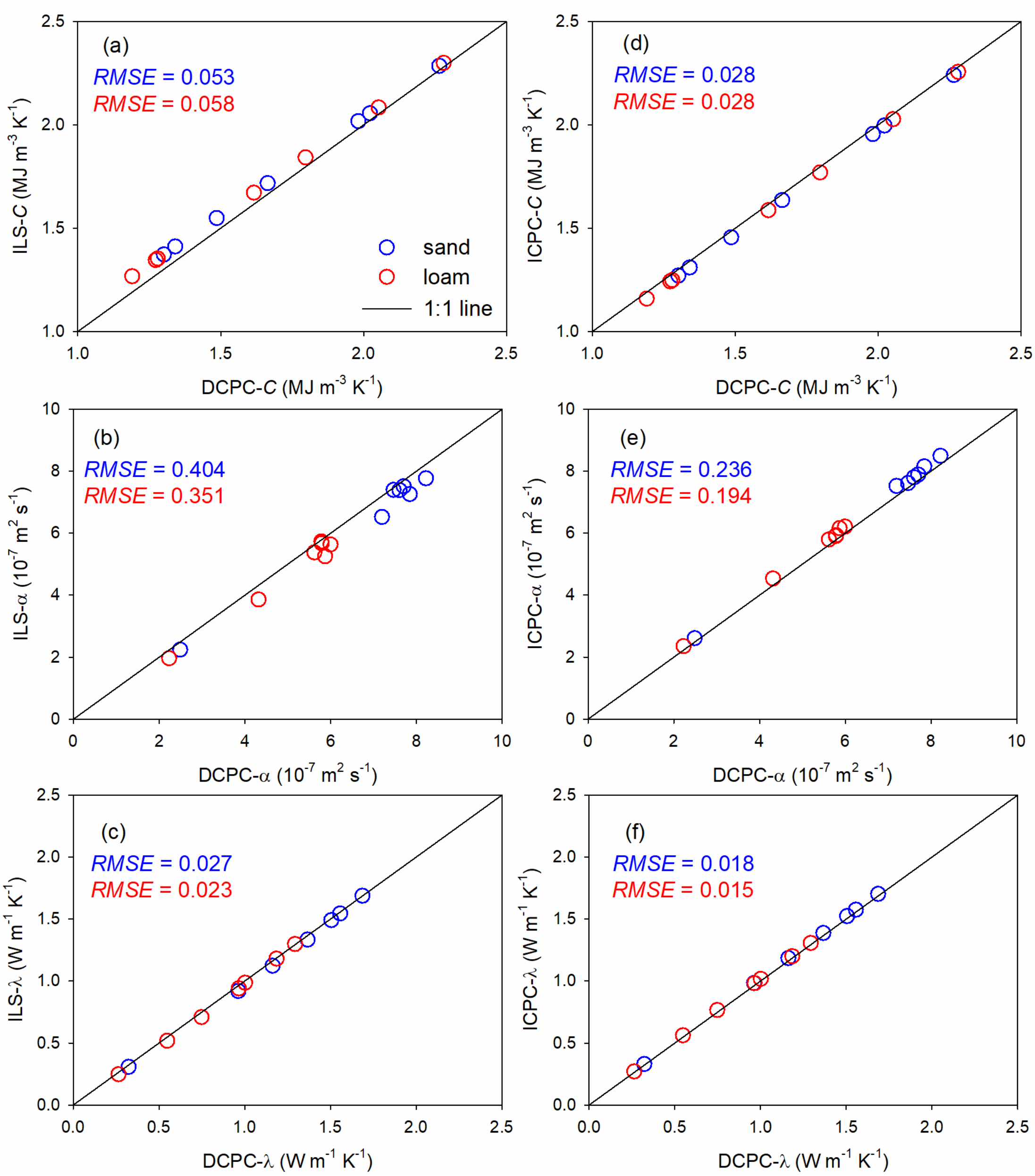

Figure 4. Relative errors (*RE*) of soil heat capacity (*C*), thermal diffusivity (α) and thermal conductivity (λ) estimated with the infinite line source (ILS) (a-c) and the identical-cylindrical-perfect-conductors (ICPC) (d-f) approaches compared to those estimated with the dissimilar-cylindrical-perfect-conductors (DCPC) approach for a sand soil and a loam soil.

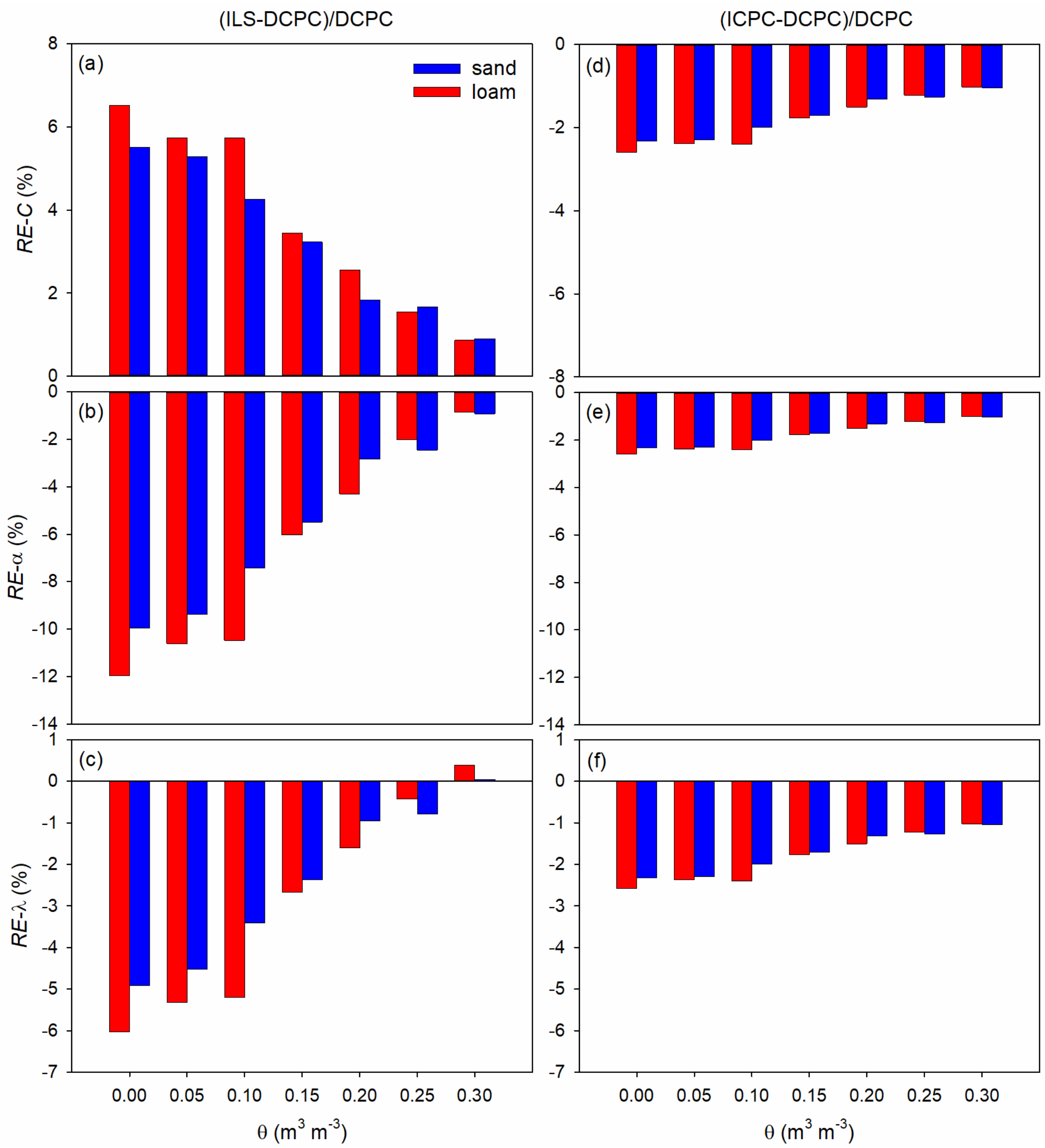

Figure 5. Relative errors (*RE*) of soil heat capacity (*C*), thermal diffusivity (α) and thermal conductivity (λ) estimated with (a) the infinite line source (ILS) approach, and (b) the identical-cylindrical-perfect-conductors (ICPC) approach vs. β_0 (the ratio between soil *C* and probe C_p) and β_2 (the ratio between soil *C* and sensing probe C_p). The solid lines are the linear regression lines between *RE* vs. β_0 and *RE* vs. β_2. The *RE*s were obtained by comparing the ILS results against ICPC results, and comparing ICPC results against those with the dissimilar-cylindrical-perfect-conductors (DCPC) approach for soils used in this study.

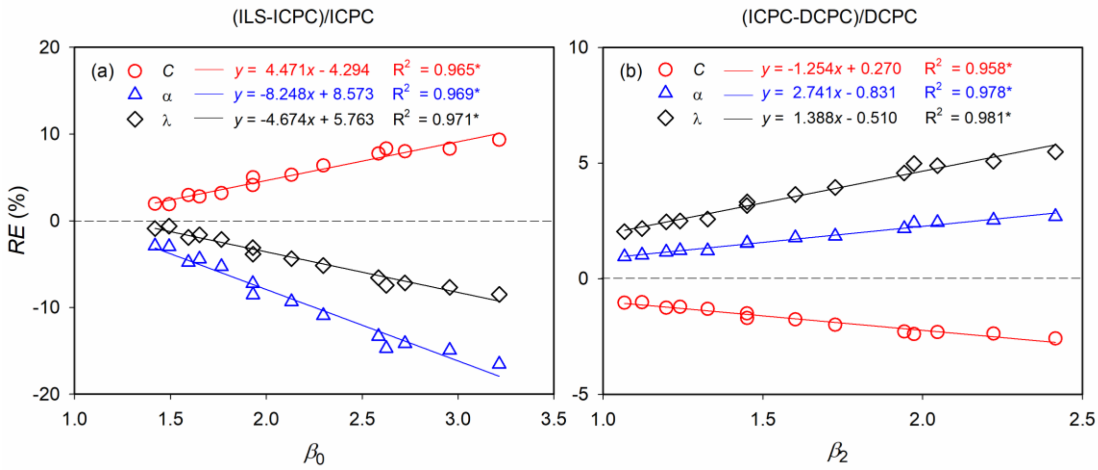

Table 1. Physical characteristics of the Peng-type sensor used in this study. For the simulation study, IP and DP scenarios are considered, representing identical or dissimilar heating and sensing probes, respectively.

Parameters	Unit	Value
IP probe radius (r_0)	mm	1.19
DP heater probe radius (r_1)	mm	1.19
DP temperature probe radius (r_2)	mm	1
Radius of epoxy filled region in heating probe (a_{eh})	mm	0.48
Radius of epoxy filled region in sensing probe (a_{es})	mm	0.75

Probe-to-probe spacing (*R*)	mm	10
Heating rate (*q'*)	W m^{-1}	45
Heating duration (t_0)	s	25
Probe length (*l*)	mm	70

Table 2. The volumetric heat capacity (*C*) and thermal conductivity (λ) of the probe materials of the Peng-type sensor used in this study.

Materials	*C* MJ m^{-3} K^{-1}	λ W m^{-1} K^{-1}
Epoxy	1.64[§]	1.04[§]
Stainless steel tube	3.77[§]	14.9[§]
Resistance wires	1.64[§]	1.04[§]
Thermocouples	1.64[§]	1.04[§]

[§] From Knight et al. (2012).